Conf-9111164--2

ANL/CP--74482

DE92 005241

SMALL ANGLE NEUTRON SCATTERING FROM NANOMETER GRAIN SIZED MATERIALS*

J. E. Epperson and R. W. Siegel
Materials Science Division
Argonne National Laboratory
Argonne, IL 60439

November 1991

DISCLAIMER

INVITED TALK presented at the International Workshop on **Studies of Magnetic Properties of Fine Particles and Their Relevance to Materials Science**, Rome, Italy, 4-8 November 1991.

*Work supported by the U.S. Department of Energy, LES-Materials Sciences, under contract #W-31-109-ENG-38.

Small Angle Neutron Scattering from Nanometer Grain Sized Materials

J. E. Epperson and R. W. Siegel

Materials Science Division, Argonne National Laboratory, Argonne, Illinois 60439 U.S.A.

Abstract

Small angle neutron scattering has been utilized, along with a number of complementary characterization methods suitable to the nanometer size scale, to investigate the structures of cluster-assembled nanophase materials. Results of these investigations are described and problems and opportunities in using small angle scattering for elucidating nanostructures are discussed.

1. INTRODUCTION

Clusters of a variety of metals and ceramics have been formed by atom evaporation and condensation in high-purity gases. The clusters are consolidated in situ under high vacuum conditions to synthesize nanophase materials, which exhibit properties that are often considerably improved relative to those of similar coarser-grained materials [1, 2]. The improved properties of these cluster-assembled nanophase materials result directly from their structures on a nanometer scale - not only their reduced grain size, but also the large percentage of their atoms in grain boundary environments. Small angle neutron scattering (SANS) has been utilized, along with a number of complementary characterization methods suitable to this size scale, to investigate the structures of nanophase materials.

In this paper, we outline the theory relevant to the small angle scattering studies done to date on nanophase systems and also discuss some areas that could provide additional information. The previous scattering experiments on nanophase materials are then reviewed and consideration is given to the future use of SANS for the study of nanostructures.

2. THEORETICAL BACKGROUND

Small angle scattering (SAS) is a low resolution technique, not sensitive to structure on an atomic scale; rather, it depends only on the size, shape, and contrast of inhomogeneities in the range from about 1-100 nm. Both X-rays and neutrons are useful for SAS investigations. For X-rays, scattering results from an electrostatic interaction of the electromagnetic wave with electrons.

There are two principal ways in which neutrons interact with the sample. In all materials the neutron is scattered by the atomic nuclei. Additionally, in ferromagnetic materials, it is scattered as well due to the interaction of the neutron's magnetic moment with that of the atom. The former gives rise to so-called nuclear scattering and the latter to magnetic scattering.

For a two-phase system, the SAS intensity can be expressed as

$$S(q) = \int_0^\infty \left[V_p(r)\, \Delta\rho\, \Phi(qr) \right]^2 N(r)\, dr, \tag{1}$$

where $q=(4\pi/\lambda)\sin\theta$ is the magnitude of the scattering vector, $V_p(r)$ is the volume of the scattering particle whose radius is r, N(r) is the distribution of particle sizes and, for spherical particles,

$$\Phi(qr) = [3\,(qr)^{-3}]\,[\sin(qr) - (qr)\cos(qr)]. \tag{2}$$

Guinier [3] showed that for non-interacting particles of arbitrary shape the central portion of the scattering profile can be approximated by a Gaussian

$$S(q) = N\,(V_p\,\Delta\rho)^2 \exp\,(-q^2\,R_g^2/3), \tag{3}$$

where R_g is the Guinier radius (or radius of gyration). However, eq. 3 is strictly valid only for particles of a single size. Most materials of interest contain a range of particle sizes, the result being that a Guinier plot [ln S(q) vs q^2] is curved; a single size parameter is thus insufficient to characterize the ensemble of scattering particles.

The origin of the curvature in the Guinier plot is apparent from eq. 1; the r^6 factor for larger particles tends to dominate the scattering profile. There are procedures for extracting particle size distributions from SAS profiles of the type discussed here; for example, the integral transform method by Brill and Schmidt [4], the linear combination of cubic spline functions by Glatter [5], and the maximum entropy method implemented by Potton and co-workers [6, 7].

The foregoing discussion is applicable in the dilute limit where interference between the scattered waves is negligible. In the more general case, Zernike and Prins [8] and Debye and Menke [9] showed that for N identical particles distributed uniformly in sample volume V, the scattering is

$$S(q) = N\,S_1(q)\left[1 + \frac{N}{V}\int_0^\infty 4\pi r^2 dr\, \{P(r) - 1\}\, \frac{\sin(qr)}{(qr)} \right], \tag{4}$$

where $S_1(q)$ is the single particle scattering function and P(r) is a radial distribution function which gives the probability of finding another particle in volume element dV at distance r from the reference particle. The second term describes the interparticle interference, the effect of which, for a liquid-like system, is to decrease the intensity in the central part of the scattering pattern. A second kind of interference has been discussed by Porod [10, 11] for very dense systems. If the probability for contact between adjacent particles excedes

that expected purely from geometrical considerations and if this enhanced contact is propagated from particle to particle, an increase in intensity in the most central part of the scattering pattern is predicted. This is referred to as gas-type scattering.

Specific models must be invoked for actual data deconvolution. Yarusso and Cooper [12] proposed a variation of a hard-sphere, liquid-like interference model for particles of a single size, and Epperson and Johnson [13] have recently extended this model to include a distribution of particle sizes. Present day computer technology renders such models viable as analytical tools.

The foregoing discussion has dealt explicitly only with the central portion of the scattering profile. However, the tail of the profile contains additional information about finer details of the microstructure. Porod [14] showed that, for randomly oriented particles of arbitrary shape but with abrupt interfaces, the intensity in the tail region obeys a definite relationship

$$S(q) = P_c\, q^{-4}, \tag{5}$$

where the Porod constant P_c is defined as the $q \to \infty$ limit of $q^4 S(q)$ and the total interfacial area is given by $P_c/2\pi(\Delta\rho)^2$. Since interparticle interference is largely confined to the very low q region, these relationships are valid even for concentrated solutions. The Porod law, however, breaks down for highly asymmetric particles, such as thin needles [15].

Not all systems possess such smooth interfaces; rather, some structures can be described by a dilation symmetry. Such fractal systems are sometimes referred to as being self similar; i.e., they remain similar in appearance as the magnification is altered over some limited range. Information about such structures is reflected in the SAS profile, but one does not obtain a specific size parameter. In particular, from the Porod regime one can extract geometric parameters related to the fractal dimension, primary particle size, and surface fractal dimension [16-18]. The power law slopes for fractal systems are generally non-integer.

A fundamentally different approach, independent of any assumptions about the microstructural details, can also be used to extract information from the scattering curves. As reviewed by Porod [11], the so-called invariant

$$Q_o = \int_0^\infty q^2\, S(q)\, dq \tag{6}$$

is directly related to the mean square fluctuation of the scattering length density. For a two-phase model in which volume is conserved,

$$Q_o = 2\pi^2\, c_1\, c_2\, (\rho_1 - \rho_2)^2, \tag{7}$$

where the c_i are volume fractions and the subscripts denote the phases.

Note that all the preceding discussions have dealt with a two-phase model. If a more complex microstructure is present, simplifying assumptions must be invoked or more sophisticated experiments must be performed. Specifically, one must find a way to vary the contrast in a controlled manner, either by isotopic substitution or by using anomalous dispersion/resonance SAS, as reviewed by Epperson and Thiyagarajan [19].

It was recounted earlier that the neutron is sensitive to the magnetic as well as the chemical microstructure due to the way it interacts with matter. For a system containing magnetic domains and when using an unpolarized neutron beam, the cross section is given by Ernst et al. [20] as

$$S(\bar{q}) = S(\bar{q})_n + S(\bar{q})_m, \tag{8}$$

where the subscripts n and m denote nuclear and magnetic, respectively. If an external, saturating magnetic field is applied, one can write

$$S(q) = S(q)_n + \sin^2 \alpha \, S(q)_m, \tag{9}$$

where α is the angle between $\bar{q}$ and $\bar{M}$, the magnetization vector. Note that this relationship affords one the possibility of making a quantitative separation of the nuclear and magnetic scattering contributions, and the components can be analyzed separately.

3. SANS STUDIES ON NANOPHASE MATERIALS

The earliest diffraction work on nanophase materials was the high angle, transmission X-ray diffraction study on iron by Zhu et al. [21]. They compared the interference function deduced from the X-ray diffraction experiment with those calculated from structural modelling. Their model assumed roughly equal volume fractions of a crystalline component and an interfacial (grain boundary) component. The interfacial component was proposed to have neither long nor short range atomic ordering. Furthermore, their modelling assumed that variations in sample density originated solely from a density deficit in the interfacial component.

On the basis of positron annihilation studies on compacted nanophase TiO_2, Siegel et al. [22] concluded that voids or pores also comprised a component of the microstructure, as indicated schematically in Fig. 1. Small angle neutron scattering from as-consolidated, nanophase TiO_2 and after selected isothermal anneals at 550°C in air was measured by Epperson et al. [23], and these data are shown in Fig. 2. Clearly, a coarsening process was taking place during the 550°C sintering anneals. They subsequently used [24] a maximum entropy method [6, 7] to extract scatterer size distributions, as shown in Fig. 3. If one, for the moment, disregards the scattering contribution due to the void/pore component, the SANS is represented by eq. 1. If one denotes the volume fraction of scattering entities as $f_v(0)$ and assumes TiO_2 of bulk density is contrasted with vacuum, one can write down an expression for the volume fraction for other contrast conditions

$$f_v = f_v(0) / (1-\delta_b)^2, \quad (10)$$

where δ_b is the fractional density (relative to bulk TiO_2) in the boundary region, again assuming theoretical bulk density for the nanophase grains. Using this expression and assuming the two-phase model, a maximum fractional density in the boundary region of about 0.63 could be assigned [23, 24]. If, on the basis of the positron annihilation experiments, one assigns the first peak in the size distribution to voids, the maximum fractional density in the boundary region was estimated to be about 0.72. Using these values and the known mean grain diameter (12 nm) from transmission electron microscopy (TEM) for these samples [22], one could estimate the average width of the grain boundaries to be about 0.5 nm, or two nearest neighbor distances. It must be emphasized, however, that these are upper limits rather than hard values for the fractional density of material in the grain boundary regions. In a parallel experiment, Eastman et al. [25] reported tentative evidence that during slow oxidation of nanophase Ti, growth occurred of a size distribution in the range of 2-3 nm radius, assumed to be TiO_2. This growth phase was associated with increased roughness of the void surfaces.

Jorra et al. [26] used SANS to study nanophase Pd. Their measurements extended down to $q = 0.019$ nm^{-1} and enhanced scattering was observed in the lowest q range. This enhanced scattering was tentatively attributed to gas-type interparticle interference [10, 11]. As a structural model, they considered nanometer sized crystallites embedded in a lower density matrix formed by incoherent boundaries. From the scattering data, they extracted a particle size distribution by the Glatter [5] method as shown in Fig. 4. The distribution was slightly asymmetrical and they reported that the major features in it could be well represented by a log-normal distribution. From the integrated SAS intensity (eq. 6), a measurement of the bulk density of the sample, and assuming the previously mentioned two-phase model, they estimated the volume fraction of the interfacial region to be about 0.7 and that its density was about half that of theoretically dense Pd. They acknowledged the possible presence of a significant void volume fraction.

For a compacted nanophase Pd sample of about 80% theoretical density, Epperson et al. [24] also used the integrated SAS intensity method and estimated the mean fractional density of the boundary region to be about 0.56. Similar analysis on a 68% theoretically dense TiO_2 nanophase compact indicated that the mean fractional density of the material in the boundary regions was only 0.21. Using the maximum entropy method, they found a particle size distribution for the Pd in reasonable agreement with that reported by Jorra et al. [26]. On the basis of these values, it was concluded that, if the boundary regions were to have reasonable densities and thicknesses, there must be a significant volume fraction of voids or pores in the sample. This conclusion is consistent with the earlier positron annihilation measurements [22] and porosimetry results reported by Hahn et al. [27]. Some of the input information necessary for such analyses, such as bulk density, is usually not known with high precision, and Epperson et al. [24] explored the effects that such errors would have on the extracted values for the volume fractions of the

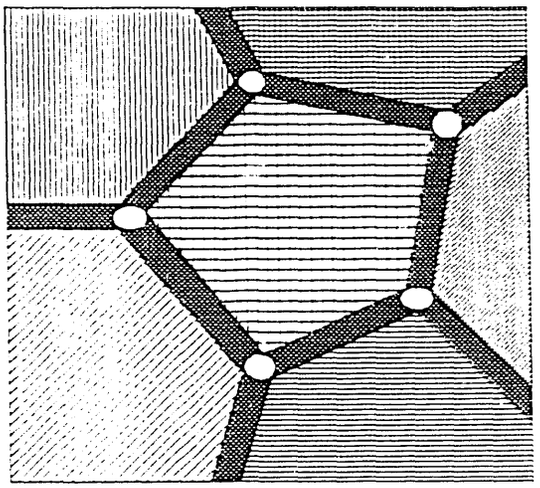

Figure 1. Schematic representation of a section through a compacted nanophase structure indicating three quintessential components: 1) fully dense nanophase grains (hatched), 2) lower-density grain boundary regions (shaded) and 3) voids or pores (unfilled circles).

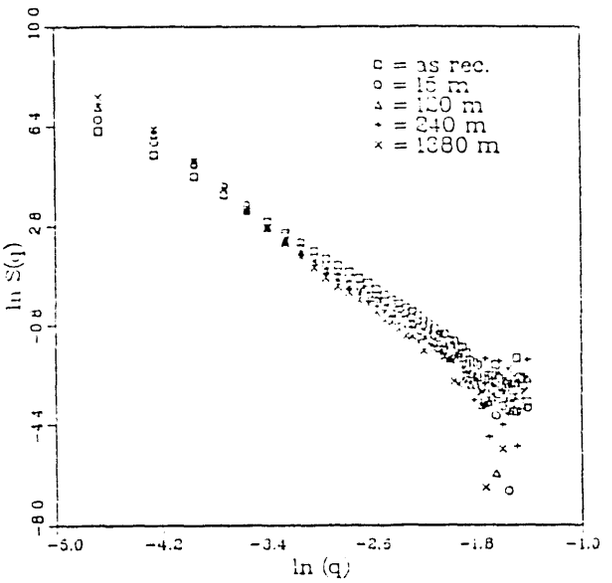

Figure 2. The effects of sintering compacted nanophase TiO_2 at 550°C: ln S(q) vs. ln q representation of the SANS for the sintering times given [23].

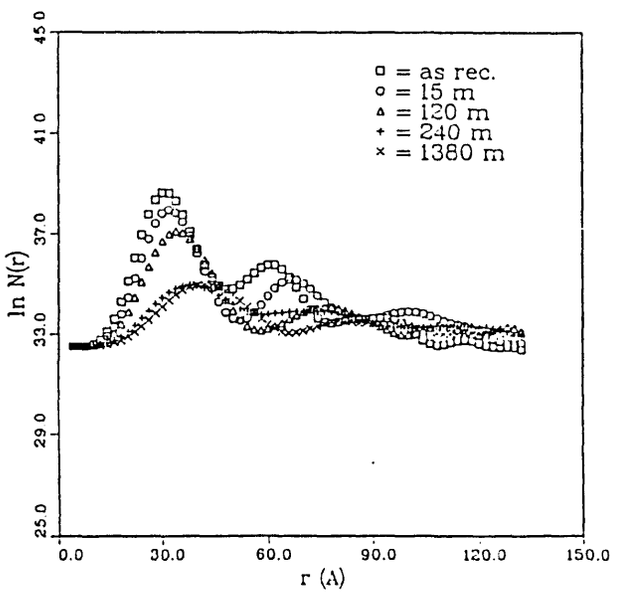

Figure 3. Semi-logarithmic display of the maximum entropy size distributions obtained for the SANS data of Fig. 2 [24].

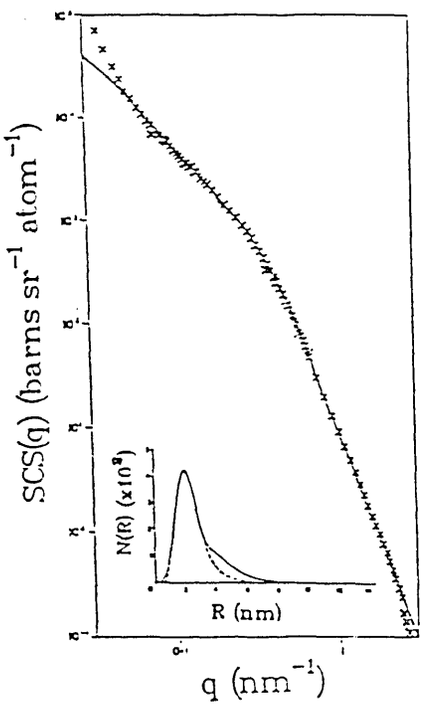

Figure 4. Compacted nanophase Pd: SANS (x) and model fitted (solid line) from the deduced log-normal size distribution (dashed line in inset) [26].

grain and interfacial regions and for the density of the grain boundary regions.

More recently, Wagner et al. [28] have also used SANS to characterize the microstructure of nanophase TiO_2 compacted at different temperatures. Enhanced scattering observed in the lowest q range was attributed to large heterogeneities (e.g., surface roughness or internal macroscopic components). They used an iterative, trial and error method, with a linear combination of four log-normal distribution functions, in an attempt to obtain information about the distribution of nanophase grains surrounded by interfacial regions and of voids. The scattering from samples compacted at elevated temperatures was significantly reduced, indicating that a large component of the SANS derives from pores and voids. After compaction at 550°C, the macroscopic density was only 8% less than that of theoretically dense rutile (TiO_2), but it could not be ascertained which part of this deficit was due to porosity and which to grain boundaries. However, the scattering from this sample was treated as a background and subtracted from that from the other samples, with the remaining scattering being treated as due to interfacial regions. From the sample compacted at 550°C, they estimated the volume fraction of the boundary regions to be 0.27 and the fractional density of these regions to be 0.70, the latter in agreement with the earlier estimates of the maximum density of the boundaries by Epperson et al. [23].

4. CONCLUSIONS

Scattering investigations have provided useful information about the microstructure of compacted nanophase materials. Some examples are the mean size of the inhomogeneities, the fractional density of material in the regions between nanophase grains, and the volume fractions of various components. However, it would be fair to observe that complementary investigations using such microscopic methods as TEM have been indispensible and that all previous SANS investigations have struggled with the fact that the microstructure consists of three phases, dense nanophase grains, boundary regions of lower density, and voids or pores. This highly concentrated, three-phase model complicates analysis of SAS data. On the other hand, data are routinely obtained in absolute cross sections and more sophisticated analysis techniques are being applied. There is reason to expect that, with carefully prepared nanophase samples and continued thought and progress in analytical methods, additional information will be forthcoming from SANS.

There are, of course, a number of nanophase materials of interest that exhibit magnetic behavior. As reviewed in a previous section, the scattering component due to magnetic domains can be treated analytically. By suitable use of an external magnetic field, one has an option of separating the magnetic and nuclear scattering. Another viable option to consider is the use of X-rays rather than neutrons. Then one would not observe, and have to deal with, the magnetic scattering, if this becomes a problem in the SANS analysis.

5. ACKNOWLEDGEMENT

This work was supported by the U.S. Department of Energy, BES-Materials Sciences, under Contract W-31-109-Eng-38.

6. REFERENCES

1. H. Gleiter, Prog. Mater. Sci. 33 (1991) 223.
2. R. W. Siegel, Ann. Rev. Mater. Sci. 21 (1991) 559.
3. A. Guinier, Ann. Physik 12 (1939) 161.
4. O. L. Brill and P. W. Schmidt, J. Appl. Phys.39 (1968) 2274.
5. O. Glatter, J. Appl. Cryst. 13 (1980) 7.
6. J. A. Potton, G. J. Daniell and D. Melville, J. Phys. D: App. Phys. 17 (1984) 1567.
7. J. A. Potton, G. J. Daniell and B. D. Rainford, J. Appl. Cryst. 21 (1988) 663.
8. F. Zernike and J. A. Prins, Z. Physik 41 (1927) 184.
9. P. Debye and H. Menke, Physik Z.31 (1930) 797.
10. G. Porod, Monatsh. Chem. 103 (1972) 395.
11. G. Porod, in Small Angle X-ray Scattering, O. Glatter and O. Kratky (eds.), Academic Press, New York (1982) 17.
12. D. J. Yarusso and S. L. Cooper, Macromolecules 16 (1983) 1871.
13. J. E. Epperson and D. J. Johnson, Mater. Res. Soc. Symp. Proc. on Kinetics of Ordering Transformations (1992) to be published.
14. G. Porod, Kolloid Z. 124 (1951) 83.
15. V. Luzzati, Acta. Cryst. 13 (1960) 939.
16. D. W. Schaefer and K. D. Keefer, Phys. Rev. Letters 56 (1986) 2199.
17. J. E. Martin, D. W. Schaefer and A. J. Hurd, Phys. Rev. A33 (1986) 3540.
18. P. W. Schmidt, in The Fractal Approach to Heterogeneous Chemistry, D. Aunir (ed.), John Wiley & Sons, New York (1989) 67.
19. J. E. Epperson and P. Thiyagarajan, J. Appl. Cryst. 21 (1988) 652.
20. M. Ernst, J. Schelten and W. Schmatz, phys. stat. sol. (a)7 (1971) 477.
21. X. Zhu, R. Birringer, U. Herr and H. Gleiter, Phys. Rev. B35 (1987) 9085.
22. R. W. Siegel, S. Ramasamy, H. Hahn, Z. Li, T. Lu and R. Gronsky, J. Mater. Res. 3 (1988) 1367.
23. J. E. Epperson, R. W. Siegel, J W. White, T. E. Klippert, A. Narayanasamy, J. A. Eastman and F. Trouw, Mater. Res. Soc. Symp. Proc. 132 (1989) 15.
24. J. E. Epperson, R. W. Siegel, J. W. White, J. A. Eastman, Y. X. Liao and A. Narayanasamy, Mater. Res. Soc. Symp. Proc. 166 (1990) 87.
25. J. A. Eastman, J. E. Epperson, H. Hahn, T. E. Klippert, A. Narayanasamy, S. Ramasamy, R. W. Siegel, J. W. White and F. Trouw, Mater. Res. Soc. Symp. Proc. 132 (1989) 21.
26. E. Jorra, H. Franz, J. Peisl, G. Wallner, W. Petry, R. Birringer, H. Gleiter and T. Haubold, Phil. Mag. B60 (1989) 159.
27. H. Hahn, J. Logas and R. S. Averback, J. Mater. Res. 5 (1990) 609.
28. W. Wagner, R. S. Averback, H. Hahn, W. Petry and A. Wiedenmann, J. Mater. Res. 6 (1991) 2193.

END

DATE
FILMED
02/13/92